Chapter 6

Catalyzed Radical Termination (CRT) in the Metal-Mediated Polymerization of Acrylates: Experimental and Computational Studies

Thomas G. Ribelli, S. M. Wahidur Rahaman, Krzysztof Matyjaszewski, and Rinaldo Poli*, 2,3

¹Department of Chemistry, Carnegie Mellon University,
4400 Fifth Avenue, Pittsburgh, Pennsylvania 15213, United States

²CNRS, LCC (Laboratoire de Chimie de Coordination),
Université de Toulouse, UPS, INPT, 205 Route de Narbonne,
BP 44099, F-31077, Toulouse Cedex 4, France

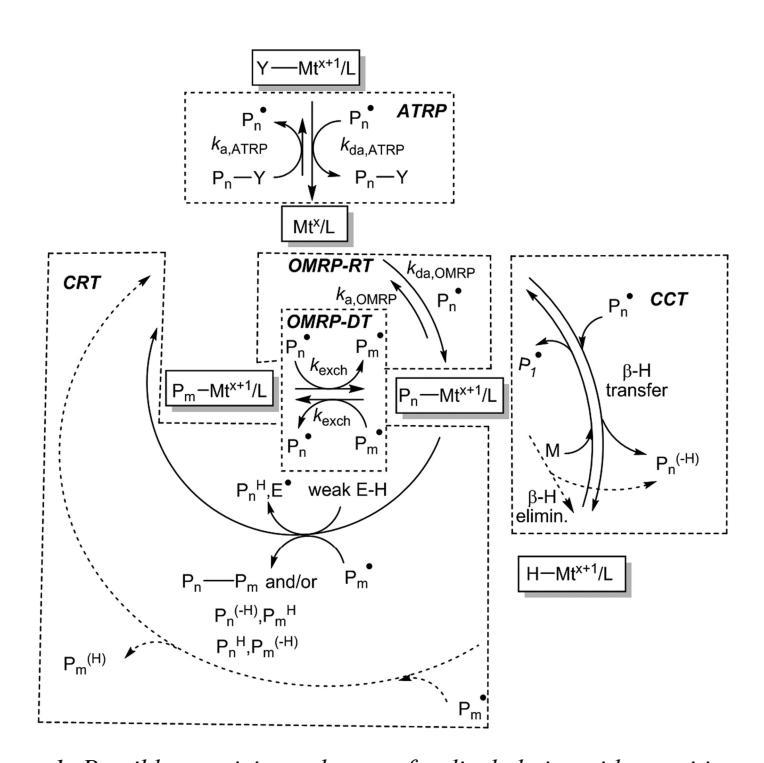
³Institut Universitaire de France, 1 rue Descartes,

75231 Paris Cedex 05, France

*E-mail:Rinaldo.Poli@lcc-toulouse.fr.

Metal complexes stabilized by appropriate ligands, particularly Cu¹/L systems, have proven powerful for the controlled polymerization of acrylates and other monomers by atom transfer radical polymerization (ATRP). The polymerization of acrylates by Cu¹/L systems, however, is haunted by interference of catalyzed radical termination (CRT), which reduces the chain-end fidelity. Other monomers do not appear to be affected by this phenomenon to any significant extent. The phenomenon appears to involve the formation of an organometallic intermediate by reversible radical trapping, as in organometallic mediated radical polymerization (OMRP). We summarize here the current knowledge and the efforts made to elucidate the CRT pathway and products.

Transition metal complexes are quite useful for macromolecular engineering by reversible deactivation radical polymerization (RDRP), notably using atom transfer radical polymerization (ATRP) (1), but also organometallic-mediated radical polymerization (OMRP) (2). However, the reactivity of organic radicals with transition metal complexes is a complex subject, with many possible reaction pathways leading to different outcomes, as summarized in Scheme 1 (3–5). The OMRP scenario, by itself, already shows complexity, because two controlling modes are possible depending on the metal coordination environment, the radical/metal stoichiometry and the metal-carbon bond strength: reversible termination (OMRP-RT) and degenerative transfer (OMRP-DT). The OMRP-RT process requires reversible homolytic cleavage of a relatively weak metal-carbon bond in the dormant species, whereas OMRP-DT requires excess radicals and an easily available coordination site on the metal atom in order to promote the reversible, rapid and degenerative associative exchange.



Scheme 1. Possible reactivity pathways of radical chains with transition metal complexes, or relevance in RDRP. Mt^x/L is a metal complex where L represents the coordination sphere and x is the formal oxidation state, Y = halogen, E = any element, and P_n^{\bullet} is a growing radical chain with degree of polymerization n. Dashed arrows are pathways that have been discarded by the experiments (see text).

If only ATRP activation/deactivation and/or OMRP activation/deactivation and/or degenerative exchange occur, a well-controlled RDRP may be obtained. Synergies between ATRP and OMRP-RT (6-8) or between the two OMRP controlling mechanisms (9-11) have been highlighted, without negative consequences (or with positive consequences) on the quality of control. However, other phenomena may interfere with controlled chain growth and it is important to understand how these occur and which factors promote them, in order to improve the polymerization control. Catalytic chain transfer (CCT) involves the same Mtx/L and Pn partners that yield OMRP-RT deactivation, but results in a β-H atom transfer to generate a dead chain with an unsaturated chain end and the metal hydride species H-Mtx/L, which then starts a new chain by delivering the H atom to monomer, see Scheme 1. Therefore, CCT and OMRP-RT deactivation are in direct competition. This is a well-known phenomenon that has its own relevance for macromolecular engineering and for industrial production (12, 13). This chapter does not deal with this nevertheless important phenomenon. Rather, it deals with the last phenomenon shown in Scheme 1, namely catalyzed radical termination (CRT). This phenomenon entails an accelerated disappearance of the radical chains, relative to spontaneous bimolecular terminations, because of the presence of the transition metal complex. In particular, it appears to have the strongest impact on the radical polymerization of acrylates and is strongly metal-dependent. It has been described so far for CuI and FeII catalysts, but not for Co^{II}, which preferentially lead to CCT or OMRP-DT when the [radical]:[Mt^x/L] ratio is greater than one. As hinted in Scheme 1, two possible pathways for CRT are possible, via the hydride complex H-Mtx+1/L and via the organometallic complex P_n-Mt^{x+1}/L and current evidence points to the latter option, as will be detailed below.

CRT Discovery and Initial Studies

The story begins with the report by Matyjaszewski and Woodworth back in 1998 (14) of the styrene and methyl acrylate polymerization under OMRP AIBN-initiated, in the presence of CuI and CuII triflates conditions, i.e. coordinated by substituted 2,2'-bipyridine (bpy) ligands and in the absence of halides. While CuII had no noticeable effect, the presence of CuI significantly retarded the MA (but not the styrene) polymerization, see upper part of Figure 1. These results were taken as evidence that, at least for styrene, the interaction between the growing polymer chain and the metal center does not contribute to chain growth control in ATRP. Otherwise stated, there is no ATRP/OMRP-RT interplay for styrene. For the MA polymerization, on the other hand, the Cu^I complex is able to act as an OMRP-RT deactivator. However, the pure OMRP-RT mechanism is not sufficient to control the polymerization because the M_n does not evolve linearly with conversion and the molecular weight distributions (MWDs) are broad, see Figure 1 (lower part). Note that this study made use of excess copper relative to initiator, rather than a catalytic amount as in later studies. It was stated that "polymer molecular weights are mostly unaffected" by the presence of Cu^I, although close inspection of Figure 1 indicates that a slight

decrease may be present. On the basis of the current knowledge, an M_n decrease is expected in the presence of CRT activity (*vide infra*). It is also worth noting that the Cu^I triflate complex was produced in situ by comproportionation of Cu^{II} triflate and Cu⁰ and, as established in a later contribution (15), Cu⁰ can also promote termination. Therefore, it is not possible to conclude on the presence of Cu^I-catalyzed termination in this system. As we now know, CRT requires formation of the organometallic intermediate, thus the absence of CRT activity for this system (or a weak one at the most) is probably the consequence of a rather weak Cu^I-PMA bond.

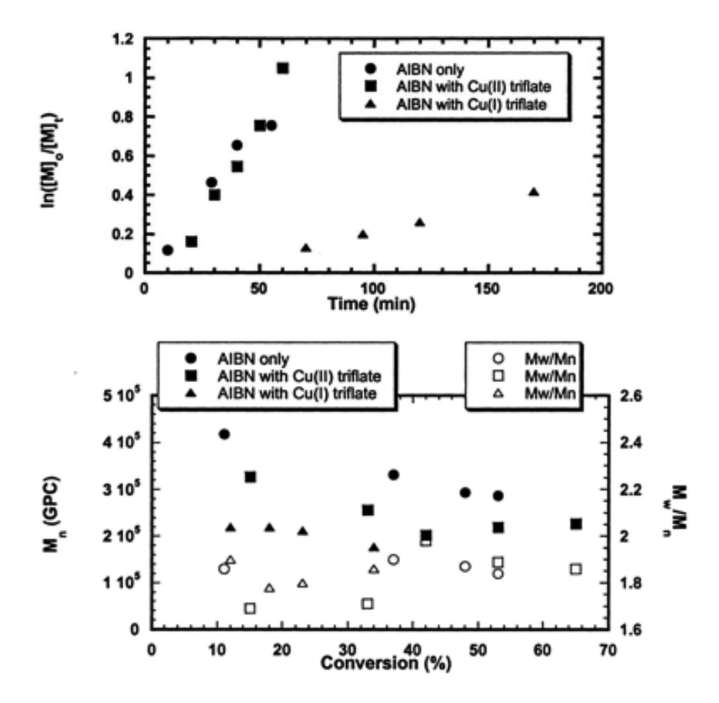
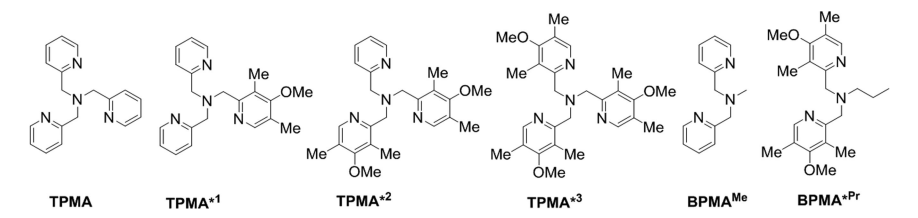


Figure 1. Kinetics and evolution of M_n and M_w/M_n with Conversion in AIBN-Initiated Polymerization of Methyl Acrylate in Toluene (3 mL) at 60°C. Conditions: MA/AIBN = 33:0.04 mmol with either no copper, or $Cu(OTf)_2$ (0.016 mmol) or $Cu(OTf)_2$ and Cu^0 (0.033 mmol of each). Reproduced with permission from ref. (14). Copyright 1998 American Chemical Society.

Clear evidence for the presence of Cu^I-CRT was obtained for the first time in a study of the butyl acrylate polymerization in the presence of [Cu^I(TPMA*³)]⁺, initiated by AIBN in anisole (once again, OMRP conditions) (16). The Cu^I complex was made in situ from [Cu^I(MeCN)₄][BF₄] and the TPMA*³ ligand, which is shown in Scheme 2 together with other ligands used in later studies. This ligand imparts a very negative reduction potential to the Cu^{II}/Cu^I redox couple, promoting OMRP-RT deactivation (as well as ATRP activation (17)). Hence, greater stability is predicted for the organometallic dormant chains [PBA-Cu^{II}(TPMA*³)]⁺.



Scheme 2. TPMA and Substituted Derivatives Used in Cu^I-CRT Investigations

Instead of controlled polymer growth by OMRP-RT, the study revealed an unexpected decrease of the polymerization rate in the presence of substoichiometric amounts of Cu^I. Furthermore, this decrease was proportional to [Cu^I]₀ (see Figure 2). Correspondingly, greater [Cu^I]₀ led to polymers with a lower M_n. PREDICI simulations were consistent with a rate-limiting reaction between Cu^I and the radical chain, followed by rapid reaction of the generated intermediate with a second radical, but could not discriminate between the hydride and the organometallic pathways shown in Scheme 1.

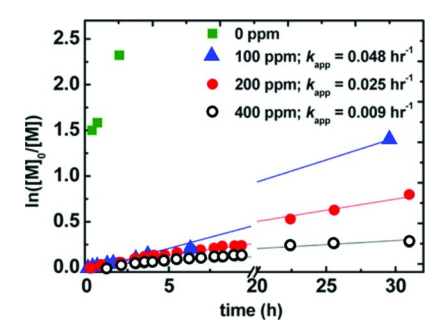


Figure 2. Kinetic plots for BA polymerizations with various [Cu^I] loadings. Conditions: [BA]:[AIBN]:[TPMA*]:[Cu^I(MeCN)₄][BF₄] = 160:0.2:0.06-0.24:0.016-0.064, [BA] = 5.6 M, 20% (v/v) anisole, T = 60 °C. Adapted with permission from ref. (16). Copyright 2012 American Chemical Society.

In subsequent work (18), Buback, Matyjaszewski *et al.* further investigated the Cu^I-CRT mechanism from the kinetic point of view using [Cu^I(TPMA)]⁺ as an ATRP activator. Normal ATRP of BA was conducted and the chain-end functionality was monitored via the accumulation of [X-Cu^{II}(TPMA)]⁺ as defined by the persistent radical effect (PRE). At 45% monomer conversion, the CEF was found to be 97% whereas 99.95% was expected if conventional bimolecular radical termination (RT) was the only source of radical termination. The difference was attributed to CRT. If the CEF resulted only from bimolecular terminations ($v_t = k_t[P_n^{\bullet}]^2$) regulated by the PRE (19), the deactivator accumulation in solution should yield a linear growth of the F(Y) function (equation 1, where $Y = [Cu^{II}/L]$ and $I_0 = [RX]_0$ and $C_0 = [Cu^I/L]_0$) (20): $F(Y) = 2k_t K_{ATRP}^2 t$. On the other hand, under the assumption that CRT occurs by the rate law $v_t = k_t c_{u(t)}[Cu^I][P_n^{\bullet}]$ and that

CRT is the dominant termination process, the deactivator accumulation should lead to the linear dependence of another function, G(Y), defined in equation 2: $G(Y) = k_{\text{LCu}(I)} K_{\text{ATRP}} t$.

$$F(Y) = \int_0^Y \frac{Y^2}{(I_0 - Y)^2 (C_0 - Y)^2} dY \qquad (1)$$

$$G(Y) = \int_0^Y \frac{Y}{(I_0 - Y)(C_0 - Y)^2} dY$$
 (2)

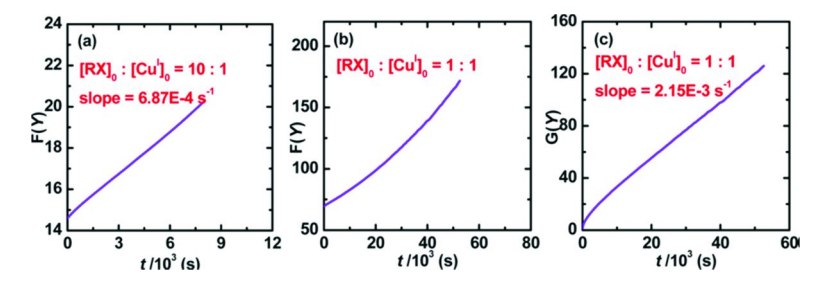


Figure 3. Time dependence of F(Y) and G(Y) in termination experiments of the model acrylate radical generated from the activation of MBrP with $Cu^{l}/TPMA$. Reproduced with permission from ref. (18). Copyright 2013 American Chemical Society.

Working with the methyl 2-bromopropionate (MBrP) initiator as a model system (in the absence of monomer) in MeCN at 25°C, a reasonably linear growth of F(Y) was observed when using a 10-fold excess of MBrP relative to the Cu^I complex (Figure 3a), indicating that conventional bimolecular radical termination dominates. However, when the reaction was conducted under stoichiometric conditions, a positive curvature of the F(Y) plot (Figure 3b) was observed, indicating that the accumulation of X-Cu^{II} was faster than expected for RT only. On the other hand, the G(Y) plot was linear after an initial negatively curved region (Figure 3c), which results from the initial non-negligible contribution of conventional bimolecular terminations. A linear G(Y) plot was also observed for the model study run with complex $[Cu^I(Me_6TREN)]^+$ as activator, as well as for the same two activators under BA polymerization conditions. The slope analysis gave the apparent CRT rate constants $k_{CRT}^{app} = 5.8 \cdot 10^3$ (TPMA) and $2.2 \cdot 10^4$ (Me₆TREN) M⁻¹ s⁻¹.

It is to be noted that these investigations were conducted in MeCN as solvent, which can potentially interfere with the termination mechanism due to the relatively weak C-H bonds. The previous study in anisole (16) used [Cu^I(MeCN)₄]⁺ as precursor, where MeCN is also present. We'll come back on this point at the end of the chapter. This contribution (18) also highlighted for the first time that CRT gives a much larger contribution to the termination

of acrylates than to those of methacrylates and styrene. This contrasts with the CCT behavior, where methacrylates are more active than acrylates, hinting to the involvement of a different key intermediate in the two mechanisms. A combination of low-temperature EPR and near-infrared investigations for the TPMA system attempted to identify this intermediate, with evidence for the accumulation of an unstable species at -40°C, but the identity of this species could not be elucidated (a more recent investigation with model radicals will be detailed in a later section).

CRT is not limited to copper(I) complexes. In a 2014 contribution (21), Schröder and Buback highlighted a Fe^{II}-catalyzed termination of acrylates, using the single-pulse pulsed laser polymerization (SP-PLP) technique to generate high concentration of photoinitiated radical chains, in combination with EPR monitoring. Comparison of the radical disappearance rate in the presence and absence of FeBr₂/[nBu₄N]Br showed a combination of conventional bimolecular and Fe^{II}-catalyzed termination. Both the secondary propagating radicals (SPR) and the midchain radicals (MCR; formed via backbiting of SPR), could be followed in time because they give two distinct EPR signals. The Fe^{II}-CRT was found to be the dominant termination pathway at high catalyst concentrations, with a rate law $v_t = k_{tFe(II)}[Fe^{II}][PBA^{\bullet}]$ and a mean value of $k_{tFe(II)} = 2.3 \cdot 10^4 \text{ M}^{-1}$ s⁻¹ at -60°C, whereas the backbiting process played a greater role at low catalyst loadings and at higher temperatures. The kinetic analysis also showed that the Fe^{II}-CRT is not an important process for MCRs and that, as also previously shown for the Cu^I-CRT, Fe^{II}-CRT plays no major role for the termination of methacrylates. Note that all these investigations were conducted in bulk monomer, not in MeCN or other solvents with weak C-H bonds. It is also useful to underline that the nature of the termination products (disproportionation or combination) was not investigated.

Hydride or Organometallic Intermediate?

As already mentioned in the previous section, the greater CRT activity for acrylates than for methacrylates, when compared to the opposite relative susceptibility of these two radicals for CCT, hints to a different key intermediate in the two processes, hence to the probable involvement of the organometallic dormant species P_n-Mt^{x+1}/L in CRT. As can be noted in Scheme 1, generation of a hydride intermediate would necessarily lead to termination by disproportionation (Disp). The pathway via the organometallic intermediate, on the other hand, could result in either Disp, combination (Comb) or chain-end saturation depending on how the organometallic species catalyzes termination (more on this later). It is therefore crucial to establish the nature of the termination products generated from CRT. We must point out here that the nature of the termination products for acrylates has been controversial, even for conventional bimolecular termination. Earlier work has pointed to the dominance of either Comb (22, 23) or Disp (24), although the former seems to attract greater favors within the community. Recent work by Asua et al. (25) concludes that the SPRs terminate preferentially by Comb, but Disp competes to a greater extent at higher temperatures following

the production of MCRs by backbiting. Additional contributions on this issue, related to the CRT mechanism, will be highlighted in the next section.

A first study of the products obtained from the CRT of polyacrylate radicals is in the above-mentioned [Cu^I(TPMA)]⁺-CRT study (18). Polystyrene (PSt-Br) and poly(methyl acrylate) (PMA-Br) ATRP macroinitiators were activated by Cu^IBr/TPMA in the absence of monomer, monitoring the Br-Cu^{II}/L deactivator accumulation by UV-visible spectroscopy. The resulting polymers were analyzed by size exclusion chromatography (SEC) and compared to the corresponding macroinitiator (see reaction sequence in Scheme 3, where the organometallic species is assumed as the key intermediate).

Scheme 3. Activation and Termination of ATRP Macroinitiators

For the PSt-Br macroinitiator, there was 50% termination after 18 h at 40°C in toluene/DMSO and the SEC analysis of the recovered polymer showed a prominent distribution at twice the molecular weight (MW) of the macroinitiator (Figure 4b), consistent with the dominance of Comb. The low M_n distribution mostly corresponds to the unreacted macroinitiator. As stated above, the Cu^I complex has negligible CRT activity for PSt radicals, which are known to preferentially terminate bimolecularly by Comb (24). For the PMA-Br macroinitiator, there was 83% termination after only 2.5 h at 25°C in MeCN and the SEC of the recovered polymer shows the absence of Comb products (Figure 4a). Note that these investigations were carried out in MeCN solution. On the basis of the widespread perception that the polyacrylates bimolecular termination leads to Comb, it was then suggested that the Cu^I-CRT of polyacrylates leads to Disp (18). Although the experimental evidence that CRT is more efficient for acrylates than for methacrylates militates against involvement of the hydride intermediate, the result of the above study is insufficient to discard the hydride pathway, because transit via this intermediate would also lead to Disp (Scheme 1).

Additional evidence in favor of the organometallic pathway was gathered via DFT calculations. A first contribution (26) evaluated the aptitude of the [Cu^I(TPMA)]⁺ complex to abstract a β-H atom from an acrylate radical, using the small model CH₃CH⁺(COOCH₃), to generate the hydride complex [H-Cu^{II}(TPMA)]⁺ and methyl acrylate. The reaction profile was compared with that of [Co^{II}(porphyrin)], a model of the bulkier tetramesitylporphyrin complex that efficiently catalyzes chain transfer to monomer. As shown in Figure 5, both complexes are predicted to favorably trap the acrylate radical to yield the OMRP-RT dormant species, (CH₃)(COOCH₃)CH-Mt^{x+1}/L. Conversely, the β-H atom transfer process, which occurs via the van der Waals adduct ^{*}CH(COOCH₃)(CH₂-H····Mt/L), is less energetically favorable and has a much higher activation barrier for the Cu^I catalyst than for the Co^{II} system. This result agrees with the known CCT activity of the Co^{II} system. Incidentally, for both

systems, the calculations also suggest that further quenching of the hydride intermediate by a radical to complete the CRT process has essentially no energetic barrier. The concentration difference ([M] >> [R $^{\bullet}$]) rationalizes the preference of [H-Co^{III}/L] to deliver the H atom to a monomer molecule to complete the CCT cycle, rather than to a radical to complete the CRT cycle.

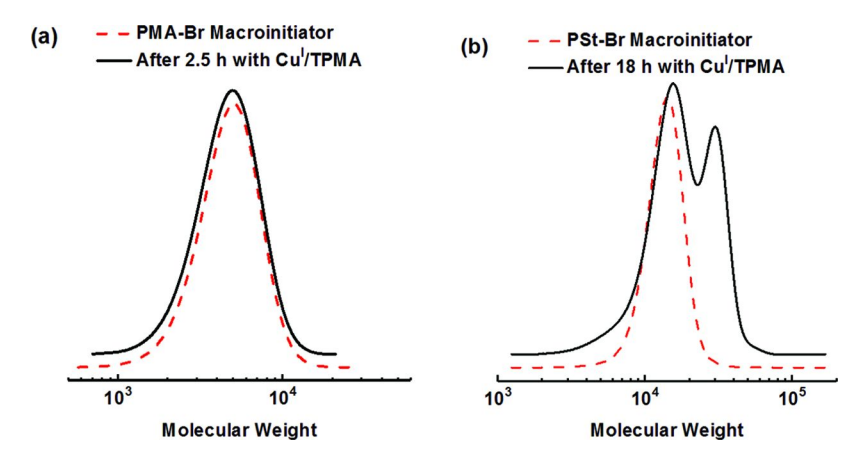


Figure 4. GPC curves of PMA-Br (a, $M_n = 4200$, D = 1.20) and PSt-Br (b, $M_n = 12000$, D = 1.10) macroinitiators and of terminated polymers after activation by $[Cu^l(TPMA)]^+$ in MeCN at 25°C for the indicated time. Reproduced with permission from the Supporting Information of ref. (18). Copyright 2013

American Chemical Society.

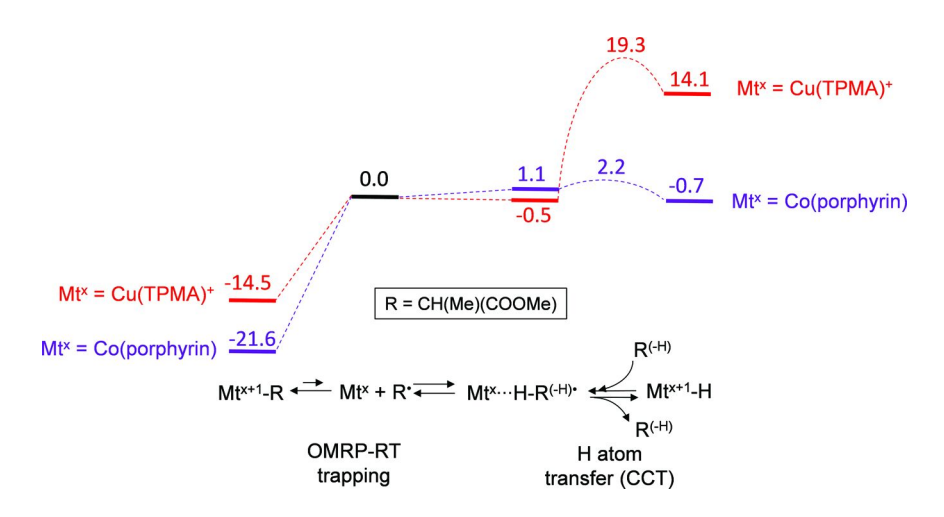


Figure 5. Gibbs energy profile for the competing OMRP-RT trapping and β -H atom transfer involving the model acrylate radical $R = CH_3CH^{\bullet}(COOCH_3)$ and complex $[Cu^I(TPMA)]^+$ or $[Co^{II}(porphyrin)]$.

The hydride intermediate hypothesis was further probed experimentally with new systems where the tetradentate TMPA ligand was replaced with a tridentate one (either BPMA^{Me} or BPMA*Pr, see Scheme 2) (27). This was motivated by the idea that β-H elimination could only occur in the presence of a vacant coordination site cis to the Cu^{II}-C bond, which would require dissociation of one of the TPMA pyridine arms. In the same contribution, a more detailed investigation was carried out for the full $[Cu^{I}(TMPA*n)]^{+}$ series of complexes (n = 0, 1, 2, 3, Scheme 2) in order to relate redox potential $(E_{1/2})$ to CRT activity. Each substitution of the pyridine ring resulted in an approximately -60 mV shift in $E_{1/2}$. By comparing the polymerization rates and polymer MWs, it was established that the CRT activity increases with more negative $E_{1/2}$, whereas the tridentate ligands yield less active catalysts: k_{CRT}^{app} (M-1 s-1) = 12 (BPMA^{Me}). 20 (BPMA*Pr), 29 (TPMA), 45 (TPMA*1), 55 (TPMA*2), 96 (TPMA*3). These results further contribute to discard the hydride pathway. In parallel, DFT calculations of the Cu^{II}-CH(CH₃)(COOCH₃) homolytic bond dissociation free energy (BDFE) revealed a linear correlation between this parameter and k_{CRT}^{app} , K_{ATRP} and the standard reduction potential of the Cu^I/Cu^{II} redox couple, see Figure 6. Interestingly, the ATRP activation equilibrium is most sensitive, the OMRP-RT activation equilibrium has intermediate sensitivity, and the CRT activity is least sensitive to the Cu^{II}/L reduction potential.

A further point of interest of that study was to reveal two limiting scenarios. For the BPMA* $^{\rm Pr}$ system, the polymer $M_{\rm n}$ scaled inversely with the catalyst loading, whereas for the TPMA-based systems the $M_{\rm n}$ decreased only marginally. Subjecting the data to kinetic analysis, the first scenario is consistent with a rate-determining formation of the organometallic intermediate, whereas the second one suggests a rate-determining reaction between the organometallic intermediate and the second radical.

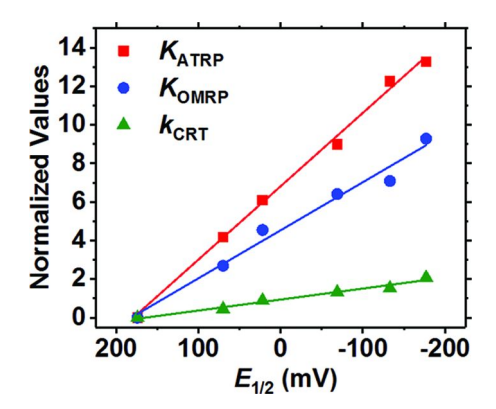


Figure 6. Relationship between $\ln K_{ATRP}$ (red squares) for MBrP in MeCN at 25 °C, $\ln K_{OMRP}$ for acrylate radical (blue circles), and \ln of apparent rate coefficient of Cu-mediated termination, $\ln k_{CRT}^{app}$ (green triangles), with the Cu^{II}/L reduction potential $E_{1/2}$. Reproduced with permission from ref. (27). Copyright 2016 American Chemical Society.

A more recent contribution by Zerk and Bernhardt has provided evidence for the generation of an organometallic intermediate, under conditions related to Cu-CRT, although not with acrylate radical models. It reports the cyclic voltammetric investigations of [Cu^{II}(TPMA)Br]Br and [Cu^{II}(Me₆TREN)X]X (X = Cl or Br) in the presence or variable amounts of ethyl 2-bromoisobutyrate (EBiB) or bromoacetonitrile (28). The [Cu^{II}(TPMA)Br]⁺ reduction in DMSO or MeCN yields an electrochemically reversible wave at E°x in the absence of RBr, but addition of the latter induces the appearance of a second irreversible reduction process at a more negative potential E°_R. This is more clearly visible as an irreversible wave when using BrCH₂CN. The same behavior is also exhibited by the voltammogram of [Cu^{II}(Me₆TREN)X]X in the presence of the corresponding XCH₂CN. The second wave is attributed to the reduction of the organometallic derivative [R-CuII/L]+, which is generated by the sequence of processes summarized in Scheme 4: (i) reduction of [X-Cu^{II}/L]⁺ to [X-Cu^I/L] at E°_X; (ii) halide dissociation to produce [Cu^I/L]⁺, (iii) ATRP activation to regenerate [X-Cu^{II}/L]⁺ and produce R[•]; (iv) R[•] trapping by the electrogenerated [CuI/L]+ complex in the diffusion layer to yield [R-CuII/L]+; (v) reduction of $[R-Cu^{II}/L]^+$ at E°_R .

The implication of radicals is consistent with the elimination of the reduction at E°R upon addition of TEMPO to the systems. The reason for the absence of a distinct wave at E°R for the EBiB substrate is consistent with the expected weaker Cu-R bond produced in that case. In other words, $1/K_{OMRP}$ = $k_{\rm da}/k_{\rm a}$ in step (iv) of Scheme 4 is too small for the EBiB system to produce a sufficiently stable organocopper(II) intermediate. The authors have attributed the irreversibility of the process at E°_R to spontaneous dissociation of the carbanion R- from the Cu^I center followed by probable protonation by traces of water. It is important to note that the addition of 17 eq. of water relative to [RX]₀ had little to no effect on the stability of the R-Cu^{II}/L intermediate, indicating stability towards hydrolysis for this intermediate on the time-scale of the electrochemical sweep. A spectroelectrochemical experiment with UV-visible detection, while maintaining a constant potential E such that $E^{\circ}_{R} < E < E^{\circ}_{X}$, was carried out on the [CuII(TPMA)Br]Br/BrCH2CN system in MeCN. At this potential, the organocopper(II) species is not reduced and accumulates in the medium. The UV-visible monitoring showed a hypochromic shift of the electronic transition and an isosbestic behavior, suggesting the relative stability of the organometallic product. The possible formation of a hydride complex, [H-Cu^{II}/L]⁺, is excluded because the •CH₂CN radical cannot furnish a β -H atom. The proposed [Cu^{II}(TPMA)(CH₂CN)]⁺ product was also characterized by EPR spectroscopy.

Scheme 4. Sequence of Reactions Occurring in the Cyclic Voltammetry of $[X-Cu^{II}/L]^+ + RX$

Combination or Disproportionation?

A series of thought-provoking contributions were published by Yamago *et al.* on the acrylate radical termination, both with and without a copper complex as a catalyst. It is more appropriate to first highlight the studies carried out in the absence of copper complexes because they are relevant for the subsequent work on CRT. The strategy used for these studies is similar the Buback/Matyjaszewski one (Scheme 3) (18) with radicals generated from well-defined macroinitiators. In this case, the radicals were generated from R_0 - M_n -TePh (M = methyl or n-butyl or t-butyl acrylate), produced by tellurium-mediated radical polymerization (TERP). Small model radicals (n = 0, 1) were also used, see Scheme 5 (29).

R₀

TePh

N

COOMe COOMe

(- PhTe)

PMA-TePh

Ph₂Te₂

R₀

R₀

R₀

N

COOMe COOMe

COOMe COOMe

Quantification
via NMR & GPC

$$(n = 0, 1, 35-400)$$

Scheme 5. Activation and Termination of TERP Macroinitiators and Small Models

The Disp/Comb ratio for the termination products was determined by SEC for the polymers or by NMR for the small model radicals. Photolysis in benzene at 25°C yielded a Disp/Comb ratio > 98/2, although a greater impact of Comb was recorder at higher temperatures (*e.g.* 52/48 for a PMA-TePh with M_n = 3200 g/mol at 120°C). In a previous publication, the same method applied to the study of polymethacrylate and polystyrene radicals (*30*) gave results (*i.e.* Disp/Comb = 67/37 and 13/87 at 100 °C for PMMA and PSt, respectively) in agreement with previous reports. The results for polyacrylates, on the other hand, are in stark contrast with some of the older and the more recent reports, as mentioned above. Even more surprisingly, in a follow-up study (*31*) the Disp/Comb ratio for the termination of PMMA and PSt radicals at various temperatures and in different solvents was found to steadily increase as the medium viscosity increased. For instance, a 97/3 Disp/Comb ratio was recorded for a PMMA-TePh macroinitiator in PEG 400 at 25°C and the same ratio was also recorded for

a PSt-TePh in polystyrene ($M_n = 96000 \text{ g/mol}$) at 60°C . Although a dominant Disp for PMMA radical is not surprising, PSt radicals were known to undergo preferred termination by Comb, under any conditions, prior to this contribution. As will be detailed below, we have found a more logical interpretation of these results, not requiring to question the established dogma on the PSt, PMMA and PMA bimolecular termination mechanisms, but before detailing this alternative interpretation, we need to come back to CRT.

In a subsequent contribution (32), Yamago *et al.* reported radical termination results using PMA-Br, PMMA-Br and PS-Br macroinitiators activated by CuBr/Cu 0 /Me $_6$ TREN, *i.e.* the same strategy of Scheme 3. It was shown that, while the PMMA and PSt radical terminations were as expected on the basis of the known bimolecular radical pathways (*i.e.* CRT played no role), the outcome of the polyacrylate radical termination was altered by the copper system. Notably, using a PMA-Br with $M_n = 2900$ and D = 1.06 in the presence of Cu 1 Br (1 equiv), Cu 0 (4 equiv), and Me $_6$ TREN (2 equiv) in toluene at 70 °C, the termination was complete in 1 h and the SEC analysis of the isolated polymer indicated a bimodal peak with a 73/27 ratio of identical and double MWDs, relative to that of the macroinitiator (Figure 7a).

This was considered surprising by the authors because, on the basis of their above-mentioned study of the termination from PMA-TePh (29), the PMA radicals should predominantly give the Disp products under these conditions. Therefore, these authors concluded that the higher MW product must result from CRT. Namely, according to these authors, Cu-CRT of polyacrylates leads to Comb, which is opposite to the conclusion of the previous study by Buback, Matyjaszewski et al. (18) Furthermore, the polymer analysis by NMR and MALDI-TOF-MS revealed that the polymer contains only saturated chain ends (PMA-H), whereas Disp would also yield an equimolar amount of macromolecules with an unsaturated chain end. The offered explanation was that, following activation, the PMA radicals are reduced to anions, most likely as an organocopper species, and then quenched to PMA-H by the moisture present in the solvent. This conclusion was further supported by an additional termination study, carried out in the presence of CH₃OD (20 equiv) under otherwise identical conditions. This experiment led to the almost exclusive formation of PMA-D (Figure 7b), as confirmed by SEC and MALDI-TOF-MS. This result also implies that the putative organocopper species is quenched faster by CH₃OD than terminated according to Cu-CRT.

Interestingly, these opposite conclusions concerning the nature of the polymer produced by Cu-CRT by Buback/Matyjaszewski (18) and by Yamago (32) were reached on the basis of the same strategy for the experiments (ATRP activation of a PMA-Br macroinitiator). However, they were based on different assumptions on the nature of the conventional bimolecular termination products: Buback, Matyjaszewski et al. considered that conventional bimolecular termination leads mostly to Comb and concluded that Cu-CRT gives Disp because they only observed Disp-like products, whereas Yamago et al. concluded that Cu-CRT leads to Comb because they also observed a significant extent of Comb, while they had found that the same radicals generated from PMA-TePh in the absence of copper yields essentially only Disp. The two studies, while following the

same strategy, are however characterized by certain differences: the Yamago study used Me₆TREN as ligand, Cu⁰ and (wet) toluene as solvent, whereas the Buback/Matyjaszewski study used TPMA as ligand, no Cu⁰ and MeCN as solvent. As already mentioned above, Cu⁰ has also been shown to promote, by itself, the termination of polyacrylate radicals (*15*), whereas the presence of protic species obviously played a role in the termination study reported by Yamago *et al.* As noted above, water had no effect on the stability of the R-Cu^{II}/L organometallic intermediate for primary and tertiary radicals on the time-scale of CV. However, the observed termination with protic species would be indistinguishable from a Cu⁰ catalyzed termination pathway which has been shown to kinetically dominate both Cu¹-catalyzed and conventional radical termination in SARA ATRP (*15*). Further investigations are needed to assess the contribution of protic species on the termination pathways.

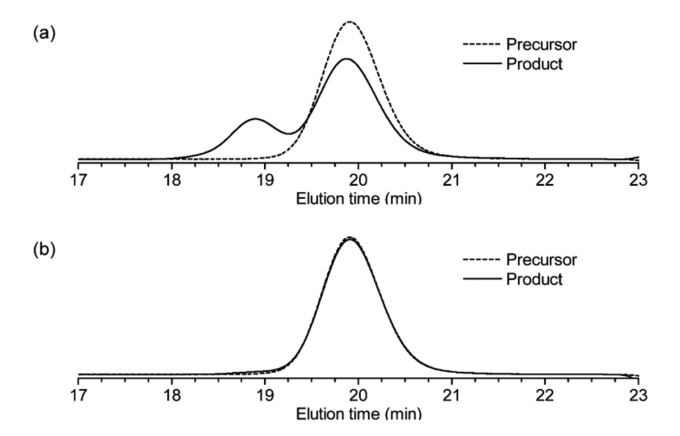


Figure 7. SEC profiles of the Cu¹/Cu⁰-mediated reaction of PMA-Br without additive (a) and with CH3OD (b). Reproduced with permission from ref. (32). Copyright 2016 American Chemical Society.

In order to elucidate the reasons for these observed differences and shed more light onto polyacrylate radical termination, with or without copper catalysts, we have run additional investigations using TPMA, TPMA*3 and Me₆TREN in carefully dried MeCN and in the absence of Cu⁰ (33). The use of Cu⁰ was avoided, not only to eliminate any contribution of Cu⁰-CRT, but also to accurately determine the extent of termination from the UV-visible monitoring of the Cu^{II} signal. In the presence of Cu⁰, the deactivator would regenerate Cu^I by comproportionation. Furthermore, in order to obtain a well-defined [Cu^I/L]⁺ activator, this was generated from [Cu^I(MeCN)₄][BF₄] rather than from Cu^IBr, because the Cu^IBr/L system is known to lead to a complex mixture of different species with different activity in ATRP (34). Finally, MeCN was preferred as solvent because it is known to disfavor [Cu^I/L]⁺ disproportionation. An additional key feature of this investigation was the use of variable amounts of added Cu^{II} deactivator, which plays no role in CRT but moderates the ATRP activation pseudo-equilibrium and thus alters the radical concentration. The ratio between

the conventional (RT) and catalyzed (CRT) termination rates is given by equation 3, showing that an increase of Cu^{II} deactivator affects the termination process by favoring CRT. The rate ratio given by equation 3 decreases with time because of the $[P_n$ -X] decrease and the [X- $Cu^{II}/L]$ increase. Thus, the relative contribution of CRT to termination keeps increasing as the process goes on.

$$\frac{rate_{RT}}{rate_{CRT}} = \frac{2k_t[p_n^*]^2}{2k_{CRT}[p_n^*][cu^I/L]} = \frac{k_t[p_n^*]}{k_{CRT}[cu^I/L]} = \frac{k_t[p_n-X]}{k_{CRT}[X-Cu^{II}/L]} K_{ATRP}$$
(3)

Using a PMA-Br macroinitiator with $M_n = 3300$ and D = 1.09, Me_6TREN as ligand, and the same [PMA-Br]₀/[Me₆TREN/Cu¹]₀ ratio (1:5) used in the previous study (32), the Cu^{II}-free termination led to quantitative (>99%) termination after 30 min at room temperature and the polymer had the SEC bimodal red trace shown in Figure 8 (left). The deconvolution of this trace, shown in Figure 8 (right), yields a 73/27 ratio of low and high MWs in very good agreement with the Yamago contribution (32). However, the polymers recovered from termination experiments run in the presence of increasing amounts of Cu^{II} deactivator, i.e. with an increased CRT contribution (Equation 3), led to a decreased proportion of the Comb product. This clearly indicates that the high molecular peak attributed by Yamago et al. to CRT coupling is actually the result of conventional termination (RT) due to the initially high radical concentration, which is caused by the high ATRP activity (high K_{ATRP}) of the Cu^I/Me₆TREN activator. The same trend (lower Comb/Disp for lower RT/CRT) was obtained when the macroinitiator was activated by Cul/ TPMA and Cu^I/TPMA*³ (33). The relative proportion of Comb product under the same concentration conditions was greater in the order TPMA < TPMA*3 < Me₆TREN. PREDICI simulations, which included consideration of backbiting, could fit the deactivator concentration and Disp fraction evolution only under the assumption that RT and CRT yield respectively Comb and Disp, whereas no fit was possible when using the opposite assumption. A minor contribution of Disp only occurs via the MCR resulting from backbiting.

It thus seems confirmed that the conventional termination of polyacrylate secondary (chain-end) radicals occurs overwhelmingly by combination. At this point, it becomes necessary to clarify the origin of the preferential disproportionation observed from the termination of polyacrylate radicals photogenerated from PMA-TePh at low temperature (29). A good hint is the observed high Disp/Comb for PSt radicals in high viscosity media (31). For a given solvent, the viscosity decreases upon raising the temperature, thus the results of the polyacrylate termination (higher Disp/Comb at lower temperature) may also be determined by the medium viscosity. The P_n-TePh photolysis generates the P_n·/PhTe· radical pair, but in order to achieve radical termination of P_n· (and dimerization of PhTe· to Ph₂Te₂, e.g. as shown for PMA-TePh in Scheme 5), the radicals must first diffuse away from the solvent cage. Radical escape from solvent cages is known to be highly viscosity dependent (35). It is thus conceivable that the Disp products arise from a side reaction between P_n· and PhTe· within the radical pair cage.

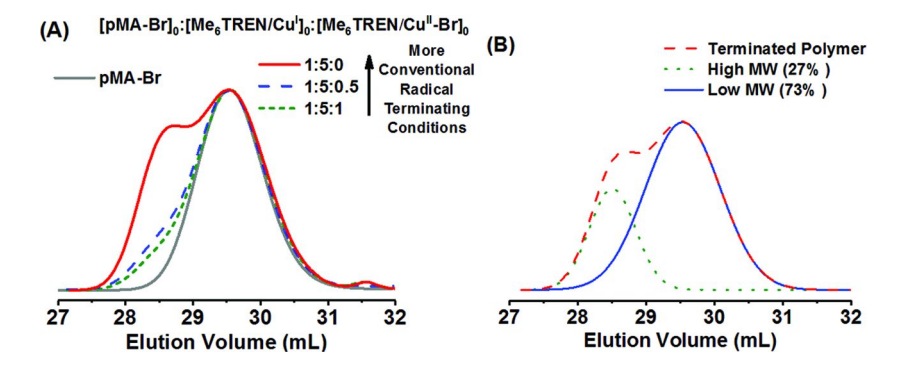


Figure 8. (A) SEC profiles of the PMA termination products obtained by the activation of PMA-Br with [Cu^I(Me₆TREN)]⁺ and variable amounts of [Cu^{II}Br(Me₆TREN)]⁺; (B) deconvolution of the SEC trace for the 1:5:0 experiment. Reproduced with permission from ref. (33). Copyright 2017 American Chemical Society.

In order to probe this hypothesis, we have investigated the Disp/Comb ratio by generating radicals in an alternative way (36). One of the model radicals used in the previously study (31), Me₂C•(COOMe), can also be generated thermally or photochemically from the commercially available diazo initiator V-601 as shown in Scheme 6. Contrary to Me₂C(COOMe)(TeMe), which forms a Me₂C•(COOMe)/PhMe• radical pair, decomposition of V-601 produces two identical radicals within the same radical pair cage, thus the termination product distribution should not greatly depend on the rate of radical escape from the cage. The results of the experiments are shown in Figure 9, in comparison with those of the previous Me₂C(COOMe)-TeMe study (31).

MeTe
$$k_{disp}$$
 k_{disp} k_{comb} k_{comb}

Scheme 6. Two Independent Ways to Generate the Same Me₂C*(COOMe) Radical

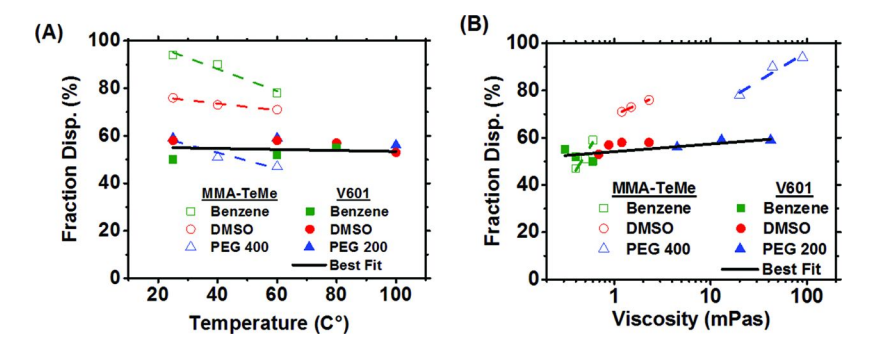


Figure 9. Fraction of disproportionation vs. (A) temperature and (B) viscosity for the isobutyryl radical in benzene. Reproduced with permission from ref. (36).

Copyright 2017 Wiley-VCH.

Quite clearly, the strong solvent, temperature, and viscosity dependence of Disp/Comb when the radical is generated from the organotellurium precursor is not present when it is generated from V-601. Notably, high viscosity media yield a lower Disp/Comb ratio for the radicals generated from V-601. The greater Disp fraction obtained in the presence of the tellanyl radical is proposed to result from a tellanyl-catalyzed process, see Scheme 7. DFT calculations on model systems, carried out with both a methacrylate and an acrylate radical, show that the two key steps, the β -H atom transfer to yield the H-TeR intermediate (a) and the H atom transfer from H-TeR to a second organic radical (b), are energetically downhill processes with very small energy barriers (36).

$$X \xrightarrow{R_1} \text{TeR} \qquad (i) \qquad \begin{cases} X \xrightarrow{R_1} \\ \text{RTe} & R_2 \end{cases} \qquad (ii) \qquad \begin{cases} X \xrightarrow{R_1} \\ \text{RTe} & X \xrightarrow{R_2} \end{cases} \qquad (iii) \qquad \begin{cases} X \xrightarrow{R_1} \\ \text{RTe} & X \xrightarrow{R_2} \end{cases} \qquad (iii) \qquad \begin{cases} X \xrightarrow{R_1} \\ \text{RTe} & X \xrightarrow{R_2} \end{cases} \qquad (iii) \qquad (iii) \qquad \qquad (iii$$

Scheme 7. Proposed Mechanism for C-Based Radical Disproportionation Catalyzed by RTe^{*}. (i) Radical pair generation; (ii) solvent cage escape; (iii) bimolecular radical termination.

Effect of the Metal Nature

We have wondered about the fundamental reason making certain metal centers (i.e. Cu^I, Fe^{II}) catalytically active in CRT, whereas Co^{II} leads to CCT or OMRP-DT when exposed to an overstoichiometric amount of radicals (cf. OMRP-DT and CRT pathways in Scheme 1). One fundamental difference between these two classes of metal centers is that those with CRT activity lead to a paramagnetic organometallic intermediate (L/Cu^{II}-P_n: S = 1/2; L/Fe^{III}-P_n: S = 5/2), whereas the cobalt system leads to a diamagnetic (S = 0) L/Co^{III}- P_n dormant species. A DFT calculation of models for these dormant species for the methyl acrylate polymerization (see Figure 10, upper part) shows that the spin density is not completely localized on the metal center. The weakness of the bond leaves a substantial amount of spin density on the alkyl chain, partially delocalized on the ester carbonyl O atom (by resonance) and on the β-H atom located anti relative to the metal atom (by hyperconjugation). The other two β-H atoms do not bear any spin density. Of course, in the real dormant species the polymer chain replaces one of the three β -H atoms, preferably the *anti* one for steric reasons, but there may be a certain probability to have the chain in a gauche position and an anti H atom. Thus, although the radical chain trapping (OMRP-RT equilibrium) disfavors RT by lowering the radical concentration, the chains radical reactivity is maintained, opening access to new pathways for termination. The dormant species can be drawn as a resonance of four limiting structures, with the unpaired electron localized on the metal, carbon, carbonyl oxygen and β -hydrogen atom, respectively (lower part of Figure 10). This leads to four possible positions of attack by the second radical chain, hence four pathways for CRT. For the diamagnetic [L/Co^{III}-P_n] system, on the other hand, the second radical may only attack a metal orbital and since the two chains are located in a relative trans position, they can only lead to degenerative exchange and not to coupling by reductive elimination.

Of the four possible pathways, the first two lead to coupling. The first one, because the new bond formed between $L/Mt^{x+1}(P_n)$ and P_m , yielding a $[L/Mt^{x+2}(P_n)(P_m)]$ intermediate, opens access to reductive elimination of P_n - P_m if the two chains occupy cis relative position in the metal coordination sphere. We can therefore imagine that control over CRT vs. OMRP-DT, even for a diamagnetic system, depends on the geometrical details of the metal coordination sphere. The second pathway involves direct bond formation between P_n and P_m . It is to be underlined that these two reactivity pathways have documented precedents, or have been proposed, in organometallic radical reactivity (37).

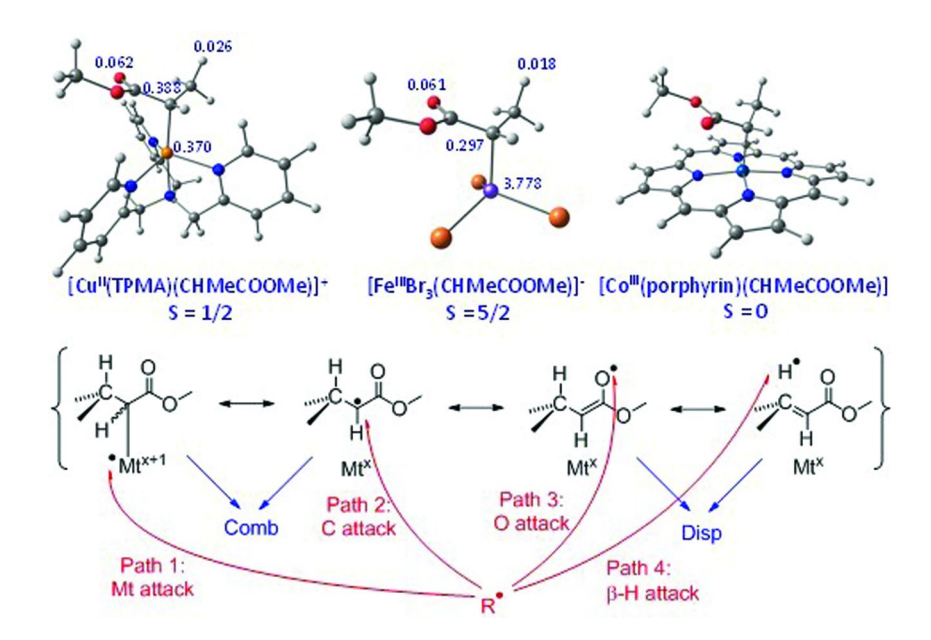


Figure 10. Upper part: Mulliken spin densities on selected atoms in the DFT-optimized geometries of $[L/Mt^{x+1}]$ -CH(CH₃)COOCH₃ ($[L/Mt^{x+1}]$ = $[Cu^{II}(TPMA)]^+$, left; $[Fe^{III}Br_3]^-$, center; $[Co^{III}(porphyrin)]$, right. Lower part: possible pathways leading to CRT.

The third pathway seems unprecedented in organometallic reactivity. However, a previous molecular dynamics computational study has shown this as a possibility for the polyacrylate termination in free-radical polymerization (29). For PMA, the C-O bonded intermediate corresponds to P_{n-1}CH₂CH=C(OMe)O-P_m, from which a facile intramolecular rearrangement, leading to the Disp products P_n-H and P_{m-1}CH=CHCOOMe, can be envisaged. Finally, the fourth pathway in Figure 10 would lead directly to the Disp products P_{n-1}CH=CHCOOMe and P_m-H. Apparently, this reaction type is also unprecedented in organometallic chemistry. Since the studies detailed in the previous sections seem to suggest that CRT leads to Disp products, the first two pathways appear excluded and the choice is restricted to the 3rd and 4th pathway in Figure 10 (however, see next section). In order to distinguish between these two possibilities, we have conceived an isotope labelling experiment. Use of a deuterated macroinitiator obtained from $CD_2=CDCOOCH_3$ (d_3 -MA), namely $p(d_3$ -MA)-Br, would lead to the same products (PMA-D and PMA-CD=CDCOOCH₃), independently of the atom being attacked (O or β -D). Therefore, the two pathways cannot be distinguished from the product analysis. However, the β-D attack is expected to be accompanied by a significant kinetic isotope effect (KIE), whereas the O-attack should not, under the assumption that the rate-determining step of CRT is the reaction between the organometallic intermediate and a second radical.

Involvement of Solvent Moisture

Before undertaking an accurate kinetic study of the isotope effect, the nature of the terminated polymers was analyzed by SEC, ¹H NMR and MALDI-TOF-MS, giving unexpected results using [CuI(TPMA)][Br] as catalyst (similar conditions used in the previous studies (18, 27, 33)). At complete termination of pMA-Br in MeCN, SEC revealed that 98% of chains had the same molecular weight as the pMA-Br macroinitiator with only 2% of chains showing coupling (Figure 11A), whereas the MALDI-TOF MS analysis of this polymer showed that it contains essentially only saturated chain-ends, without unsaturations (Figure 11B). This result is similar to that reported by Yamago et al. for their study in wet toluene, thus we reasonably wondered about the presence of water in the MeCN solvent, although we also considered the possible involvement of the weak C-H bond of MeCN in a hydrogen atom transfer (HAT) mechanism (Scheme 1). A termination of pMA-Br in d_3 -MeCN and DMF under the same conditions also showed only pMA-H saturated chains with only a small presence of coupled chains and the termination of $p(d_3-MA)$ -Br gave $p(d_3-MA)$ -H with no unsaturated species or deuterium-capped chains, as indicated by MALDI-TOF-MS. This excludes the HAT mechanism and confirms that residual solvent moisture may play an important role under these diluted conditions (needed to accurately measure the Cu^{II} concentration by UV-visible spectroscopy).

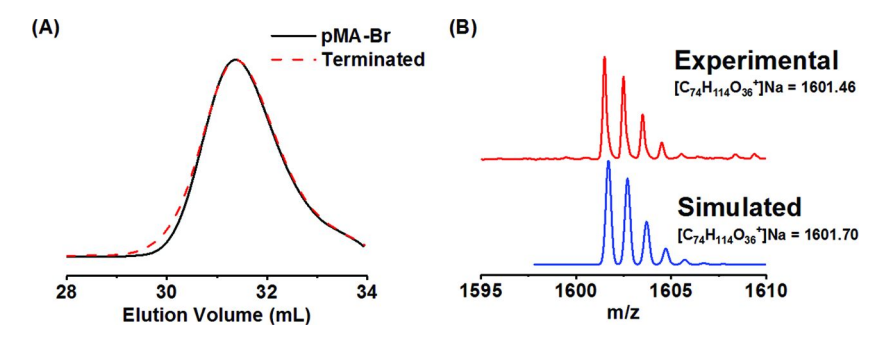
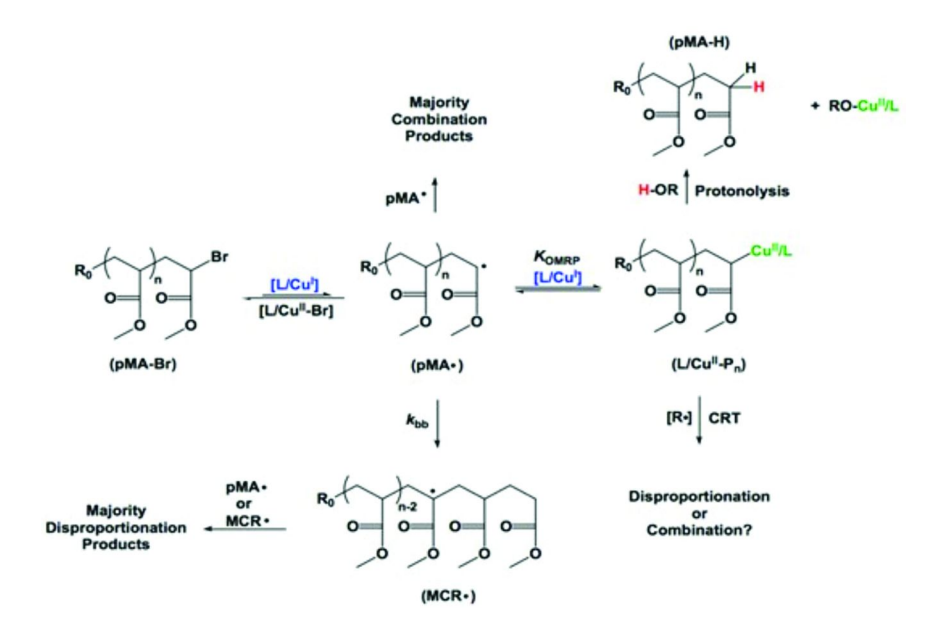


Figure 11. Termination of pMA-Br in A) MeCN or B) d_3 -MeCN under the initial conditions [pMA-Br]:[CuBr]:[TPMA] = 1:2:2.1 at $25^{\circ}C$; $[pMA-Br]_0 = 10$ mM.

Additional termination experiments were also conducted with the ATRP initiator methyl 2-bromopropionate (MBrP) as an acrylate model under the same conditions as the polymeric analog in MeCN. This species does not undergo backbiting, allowing to remove one possible complication. The NMR analysis of the products in both d_3 -MeCN and d_7 -DMF showed that 80% of the terminated radicals were coupled, as a result of bimolecular RT, while the rest were saturated, CH₃CH₂COOMe. There was no evidence of disproportionation either from vinyl peaks or the formation of oligomers. In this case, possibly because of a different amount of residual moisture in the solvent, the impact of hydrolytic decomposition

was lower. Also of relevance is the absence of succinonitrile, NCCH₂CH₂CN, and of the coupling product between the cyanomethyl and acrylate radicals, CH₃CN(CH₂CN)COOMe, once again discarding any Cu-catalyzed HAT from the solvent (Scheme 1). These results may suggest that CRT is either less effective for the unimer radical generated from MBrP, or also leads preferentially to combination. Note also that the bimolecular termination rate constant, k_t , is 10 times slower for polymeric radicals than for small molecules (38). Incidentally, this result further supports the notion that the RT of acrylates proceeds via combination (33).

These results clearly show that there are multiple pathways for the termination of acrylate radicals in ATRP: 1) bimolecular termination of chain-end radicals, predominantly by combination; 2) bimolecular termination of mid-chain radicals (from backbiting), mostly by disproportionation; 3) CRT, proceeding via the L/Cu^{II}-P_n organometallic species by a yet unknown mechanism and 4) hydrolysis of the L/Cu^{II}-P_n species by adventitious moisture. These pathways are summarized in Scheme 8. The intimate details of the Cu-CRT are currently being investigated.



Scheme 8. Pathways of Acrylate Radical Termination in Copper-Catalyzed ATRP

Critical Evaluation of CRT

The recent discovery of the moisture involvement in the Cu¹-CRT studies, detailed in the previous section, leads us to reconsider all previous conclusions reached by ourselves and others on the CRT mechanism and on the nature of the dead chains (Comb *vs.* Disp). Most previous studies of CRT carried out under

both catalytic and stoichiometric conditions in our own laboratories were done in the presence of MeCN, either as solvent or from the Cu¹ salt (16, 18, 27, 33). The MWD of the terminated polymers obtained from the activation of P_n-Br under stoichiometric conditions shows that the major component has a MWD identical to that of the macroinitiator, initially interpreted as resulting from Disp (18). In light of the more recent findings by Yamago et al. (32) and ourselves (previous section), all those MWDs were probably resulting from a stoichiometric hydrolytic decomposition of the organocopper(II) intermediate with the sole formation of P_n-H. The existence of CRT, however, is clearly proven by the polymerization studies carried out under OMRP conditions with catalytic quantities of copper complex and must lead to bimolecular radical products (Disp or Comb). The presence of adventitious water has no effect on Cu-catalyzed ATRP, it only consumes the copper catalyst by hydrolyzing the organocopper(II) intermediate to generate a putative Cu^{II}(OH) species, which may however be reinjected into the ATRP system in the presence of suitable reducing agents. The Fe^{II}-CRT of polyacrylate radicals reported by Buback et al., investigated in bulk monomer, also proves the presence of CRT. Unfortunately, that study gave no information on the product MWD (21). Clearly, more investigations are necessary on the nature of the polymer (MWD) obtained in the presence of stoichiometric amounts of activator, under conditions in which moisture is completely avoided or at least drastically reduced relative to copper, in order to fully elucidate the CRT mechanism (these experiments are ongoing in our laboratories).

Conclusion

The present account outlines the complicated scenario related to the important CEF problem in the ATRP of acrylate monomers, resulting from radical terminations. A contribution of Cu-CRT has clearly been illustrated by recent reports. Progress in this area has been somewhat polluted by contrasting evidences and subsequent debates on the nature of the termination products from both the spontaneous bimolecular RT and CRT (combination or disproportionation), as well as by water contamination of the solvents, leading to hydrolytic decomposition of the organometallic intermediate. spontaneous bimolecular RT was shown to consist of combination for secondary chain-end radicals and disproportionation for tertiary mid-chain radicals that result from back-biting processes, the contribution of solvent moisture in the generation of saturated chains during stoichiometric experiments has haunted so far the determination of the Cu-CRT mechanism. An initially suspected HAT from the MeCN solvent has not been substantiated and does not seem to occur to a significant extent. We hope that the present account, as well as further investigations currently ongoing in our laboratories, will contribute to elucidate all intimate details of the radical termination in the acrylate ATRP, allowing optimization of the catalyst and of the operating conditions in order to obtain polymers with the highest possible CEF.

Abbreviations

AIBN Azobis(isobutyronitrile)

ATRP Atom transfer radical polymerization

BA *n*-Butyl acrylate

BDFE Bond dissociation free energy
BPMA Bis(2-pyridylmethyl)amine
CCT Catalytic chain transfer
CEF Chain-end functionality

Combination Combination

CRT Catalyzed radical termination
DFT Density functional theory

Disp Disproportionation

EBiB Ethyl 2-bromoisobutyrrate
HAT Hydrogen atom transfer
KIE Kinetic isotope effect
MA methyl acrylate

MALDI-TOF- Matrix-assisted laser desorption ionization – time-of-flight –

MS mass spectrometry

MBrP Methyl 2-bromopropionate

MCR Midchain radical

Me₆TREN tris(2-dimethylaminoethyl)amine

MW Molecular weight

MWD Molecular weight distribution

MMA methyl methacrylate

NMR Nuclear magnetic resonance

OMRP-RT Organometallic-mediated radical polymerization by

reversible termination

OMRP-DT Organometallic-mediated radical polymerization by

degenerative transfer

PEG Poly(ethylene glycol)

RDRP-DT Reversible deactivation radical polymerization

SEC Size exclusion chromatography SPR Secondary propagating radical

St Styrene

TPMA tris(2-pyridylmethyl)amine

Acknowledgments

We thank the Centre National de la Recherche Scientifique (CNRS) for funding our collaborative project in the form of a PICS grant (No. 6782, 2015-17) and then for the establishment of a "Laboratoire Internation Associé" (LIA) called "Laboraty of Coordination Chemistry for Controlled Radical Polymerization" (2018-21). The computational work was granted access to the HPC resources of IDRIS under the allocation 086343 made by GENCI (Grand Equipment National de Calcul Intensif) and to the resources of the CICT (Centre Interuniversitaire de Calcul de Toulouse, project CALMIP). Additional support from the French

Embassy in Washington D.C. (Chateaubriand fellowship to TGR), from the ANR grant FLUPOL (ANR-14-CE07-0012, 2015-18), from the Mational Science Foundation (CHE 1707490), and from the Institut Universitaitre de France (IUF) is also gratefully acknowledged.

References

- 1. Matyjaszewski, K. *Macromolecules* **2012**, *45*, 4015–4039.
- 2. Poli, R. Organometallic Mediated Radical Polymerization. In *Reference Module in Materials Science and Materials Engineering*; Elsevier, 2016.
- 3. Poli, R. Angew. Chem., Int. Ed. 2006, 45, 5058–5070.
- 4. Poli, R. Eur. J. Inorg. Chem. 2011, 1513–1530.
- 5. Poli, R. Chem. Eur. J. **2015**, 21, 6988–7001.
- Le Grognec, E.; Claverie, J.; Poli, R. J. Am. Chem. Soc. 2001, 123, 9513–9524.
- 7. Braunecker, W. A.; Brown, W. C.; Morelli, B.; Tang, W.; Poli, R.; Matyjaszewski, K. *Macromolecules* **2007**, *40*, 8576–8585.
- 8. Poli, R.; Shaver, M. P. Inorg. Chem. 2014, 53, 7580-7590.
- Wayland, B. B.; Peng, C.-H.; Fu, X.; Lu, Z.; Fryd, M. Macromolecules 2006, 39, 8219–8222.
- Maria, S.; Kaneyoshi, H.; Matyjaszewski, K.; Poli, R. Chem. Eur. J. 2007, 13, 2480–2492.
- 11. Santhosh Kumar, K. S.; Gnanou, Y.; Champouret, Y.; Daran, J.-C.; Poli, R. *Chem. Eur. J.* **2009**, *15*, 4874–4885.
- 12. Gridney, A. A.; Ittel, S. D. Chem. Rev. 2001, 101, 3611–3659.
- 13. Slavin, S.; McEwan, K.; Haddleton, D. M. Cobalt-Catalyzed Chain Transfer Polymerization: A Review. In *Polymer Science: A Comprehensive Reference*; Matyjaszewski, K., Möller, M., Eds.; Elsevier BV: Amsterdam, 2012; Vol. 3, pp 249–274.
- 14. Matyjaszewski, K.; Woodworth, B. E. *Macromolecules* **1998**, *31*, 4718–4723.
- Krys, P.; Wang, Y.; Matyjaszewski, K.; Harrisson, S. Macromolecules 2016, 49, 2977–2984.
- Schröder, K.; Konkolewicz, D.; Poli, R.; Matyjaszewski, K. *Organometallics* 2012, 31, 7994–7999.
- 17. Kaur, A.; Ribelli, T. G.; Schroeder, K.; Matyjaszewski, K.; Pintauer, T. *Inorg. Chem.* **2015**, *54*, 1474–1486.
- 18. Wang, Y.; Soerensen, N.; Zhong, M.; Schroeder, H.; Buback, M.; Matyjaszewski, K. *Macromolecules* **2013**, *46*, 683–691.
- 19. Fischer, H. Chem. Rev. **2001**, 101, 3581–3610.
- Tang, W.; Tsarevsky, N. V.; Matyjaszewski, K. J. Am. Chem. Soc. 2006, 128, 1598–1604.
- 21. Schroeder, H.; Buback, M. Macromolecules 2014, 47, 6645–6651.
- 22. Ayrey, G.; Humphrey, M. J.; Poller, R. C. Polymer 1977, 18, 840–844.
- 23. Szablan, Z.; Junkers, T.; Koo, S. P. S.; Lovestead, T. M.; Davis, T. P.; Stenzel, M. H.; Barner-Kowollik, C. *Macromolecules* **2007**, *40*, 6820–6833.

- 24. Bamford, C. H.; Jenkins, A. D. *Nature* **1955**, *176*, 78–78.
- 25. Ballard, N.; Hamzehlou, S.; Ruiperez, F.; Asua, J. M. *Macromol. Rapid Commun.* **2016**, *37*, 1364–1368.
- 26. Rahaman, S. M. W.; Matyjaszewski, K.; Poli, R. *Polym. Chem.* **2016**, *7*, 1079–1087.
- 27. Ribelli, T. G.; Rahaman, S. M. W.; Daran, J.-C.; Krys, P.; Matyjaszewski, K.; Poli, R. *Macomolecules* **2016**, *49*, 7749–7757.
- 28. Zerk, T. J.; Bernhardt, P. V. Inorg. Chem. 2017, 56, 5784–5792.
- 29. Nakamura, Y.; Lee, R.; Coote, M. L.; Yamago, S. *Macromol. Rapid Commun.* **2016**, *37*, 506–513.
- 30. Nakamura, Y.; Yamago, S. *Macromolecules* **2015**, *48*, 6450–6456.
- 31. Nakamura, Y.; Ogihara, T.; Hatano, S.; Abe, M.; Yamago, S. *Chem. Eur. J.* **2017**, *23*, 1299–1305.
- 32. Nakamura, Y.; Ogihara, T.; Yamago, S. ACS Macro Lett. 2016, 5, 248–252.
- 33. Ribelli, T. G.; Augustine, K. F.; Fantin, M.; Krys, P.; Poli, R.; Matyjaszewski, K. *Macromolecules* **2017**, *50*, 7920–7929.
- 34. De Paoli, P.; Isse, A. A.; Bortolamei, N.; Gennaro, A. *Chem. Commun.* **2011**, 47, 3580–3582.
- 35. Khudyakov, I. V. Res. Chem. Intermed. 2013, 39, 781–804.
- 36. Ribelli, T. G.; Rahaman, S. M. W.; Matyjaszewski, K.; Poli, R. *Chem. Eur. J.* **2017**, *23*, 13879–13882.
- 37. Crossley, S. W. M.; Obradors, C.; Martinez, R. M.; Shenvi, R. A. *Chem. Rev.* **2016**, *116*, 8912–9000.
- 38. Fischer, H.; Radom, L. Angew. Chem., Int. Ed. **2001**, 40, 1340–1371.